Talanta 233 (2021) 122506

Contents lists available at ScienceDirect

Talanta

journal homepage: www.elsevier.com/locate/talanta

Detecting cancer cells with a highly sensitive LbL-based biosensor

Abilene Rodrigues Correia [a], Isabella Sampaio [a,*], Edson José Comparetti [a], Nirton Cristi Silva Vieira [a,b], Valtencir Zucolotto [a]

[a] GNano – Nanomedicine and Nanotoxicology Group, São Carlos Institute of Physics, University of São Paulo, CP 369, 13560-970, São Carlos, SP, Brazil
[b] Institute of Science and Technology, Federal University of São Paulo, 12231-280, São José dos Campos, SP, Brazil

ARTICLE INFO

Keywords:
Tumor cells detection
Layer-by-layer self-assembly
Electrochemical biosensor
Folic acid

ABSTRACT

Early diagnosis of cancer is crucial for therapeutic methods to be more effective and to decrease the mortality rate due to this disease. Current diagnostic methods include imaging techniques that require expensive equipment and specialized personnel, making it difficult to apply them to many patients. To overcome these limitations, many biosensors have been developed to monitor cancer biomarkers. Here, we report on the electrochemical biosensor for selective detection of tumor cells using a simple and low-cost methodology. Layer-by-layer (LbL) self-assembly was used to modify indium tin oxide (ITO) electrodes with alternating layers of polyallylamine hydrochloride (PAH) and folic acid (FA), which binds to overexpressed folate receptors alpha (FRα) in tumor cells. The LbL-based biosensor showed high sensitivity in detecting cervical cancer cells (HeLa cells) using cyclic voltammetry (CV) and electrochemical impedance spectroscopy (EIS). A linear dependence with the logarithm cell concentration was observed and excellent detection limits were found, 4 cells mL^{-1} and 19 cells mL^{-1} for EIS and CV measurements, respectively. The developed biosensor also presented great reproducibility (RSD = 1.7%) and repeatability (RSD = 1.8%). The selectivity was confirmed after the biosensor interaction with healthy cells (HMEC cells), which did not produce significant changes in the electrochemical signals. Furthermore, it was demonstrated that selective detection of tumor cells occurs via an interaction with FA. The LbL-based biosensor provides a simple, accurate, and cost-effective platform to be applied in the early diagnosis of cancer.

1. Introduction

Cancer is the second leading cause of death worldwide, being responsible for more than 9.5 million deaths in 2018, according to the World Health Organization (WHO) [1,2]. Early diagnosis is crucial to provide more effective treatment and increase the survival rate of patients, especially in the most severe types of cancer. Currently, diagnosis is performed by imaging techniques such as computerized tomography, magnetic resonance imaging, and X-ray radiography [3,4]. However, these techniques require complex and costly equipment that needs to be operated by specialized people [4]. Therefore, the development of simple and low-cost diagnostic methods for detecting tumor cells can contribute to the early diagnosis [5], reducing the cancer costs for healthcare systems.

Folate receptors (FRs) are glycoproteins located on the cell membrane that bind folic acid (FA), an essential vitamin for cell proliferation, and mediate its endocytosis [6]. FRs present four isoforms, which have different expression levels in cells [6]. Several studies have identified the folate receptor alpha (FRα) isoform as a potential tumor biomarker [7,8]. In healthy epithelial cells, FRα is expressed at normal levels and is preferably located on the apical membrane, oriented towards the lumen [9]. However, in epithelial tumors with high proliferation activity, for example, cervical and ovarian carcinomas, FRα is overexpressed on the cell membrane surface [10]. Different methods have been employed for FRα quantification in tissue samples such as proteomics assays [8], fluorescence imaging [11], and positron emission tomography [12]. However, these methods present some disadvantages, including complex and time-consuming procedures and the use of toxic radioligands [13,14].

Biosensors represent an attractive platform for cancer diagnosis because they enable simple, fast, and accurate monitoring of biomarkers [15]. Biosensors using different strategies have been developed for cancer diagnosis [5,14,16–19]. Ni et al. reported an immobilization-free electrochemical biosensor for the FRs detection in cervical cancer cells

* Corresponding author.
E-mail address: isabellasampaio@ymail.com (I. Sampaio).

https://doi.org/10.1016/j.talanta.2021.122506
Received 5 April 2021; Received in revised form 30 April 2021; Accepted 5 May 2021
Available online 11 May 2021

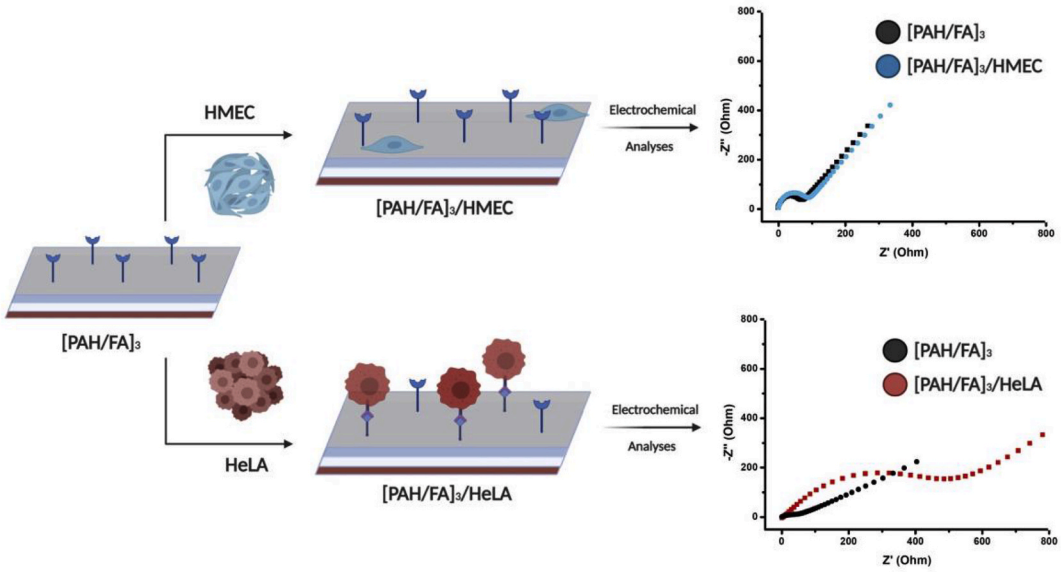

Scheme 1. Schematic illustration of the detection of tumor cells by the LBL biosensor.

[13]. Folic acid molecules attached to ferrocene modified oligonucleotides were used as capture probes. These probes were pre-incubated with tumor cells and then with the exonuclease I enzyme (EXO1). The reaction mixture was subjected to electrochemical measurements using a negatively charged indium tin oxide (ITO) as the working electrode. In the absence of FRs, EXO 1 degrades the probes, releasing the electroactive ferrocene that accumulates on the ITO surface. However, the probes are protected from degradation when bound to FRs, which decreases the current generated by free ferrocenes. A linear relationship between the logarithm of Hela cells concentration and the decrease in electrochemical signal was demonstrated [13]. Recently, Du et al. developed an electrochemical cytosensor based on FRs detection in which zirconium metal-organic frameworks modified with FA molecules were immobilized on gold electrodes. The biosensor detected a breast tumor cell line with good reproducibility and selectivity, reaching a limit of detection (LOD) of 10 cells/mL [16]. Although these biosensors have shown promising results for cancer detection, a simpler and lower-cost methodology is still required for the biosensors to be fabricated on a large scale and employed in healthcare systems.

Layer-by-layer (LbL) assembly is a very attractive technique for the construction of multilayer films [20]. Conventionally, the growth of the films is performed by the sequential immersion of an electrode platform into solutions containing oppositely charged molecules [21,22]. For instance, negatively charged biomolecules can be immobilized on a pre-coated electrode with a cationic polymer through electrostatic interactions [23]. Therefore, the LbL technique is advantageous for biosensors fabrication because it provides a simple and low-cost methodology in addition to preserving the function of biomolecules and allowing the control of the roughness and thickness of the layers [24,25]. Some LbL-based biosensors have been reported for the detection of cancer biomarkers including circulating tumor DNA [2], peptides [26], and glycoproteins [4,27]. To assembly LbL films, ITO is an excellent substrate due to its good conductivity, low capacitive current, and because it represents a low-cost alternative to the conventional gold and platinum electrodes [28].

We previously reported the development and optimization of a simple and low-cost electrochemical biosensor using the LbL technique for FRα molecule detection in buffer solutions [29]. The growth of multilayer films was performed by alternating immersion of ITO electrodes in polyallylamine hydrochloride (PAH) and FA solutions. A linear relationship between the biosensor electrochemical response and FRα concentration was achieved, demonstrating its potential application for detecting carcinomas. Herein, we evaluated the performance of the LbL biosensors in the quantification of FRα positive tumor cells, using a cervical cancer cell line (HeLa cells) as a model. The selectivity of the biosensor was investigated through measurements on normal human mammary epithelial cells (HMEC). To determine whether the detection of HeLa cells is due to the FA-FRα interactions, LbL films replacing FA with the poly(acrylic acid) (PAA) polymer were constructed and subjected to detection measurements. Our results showed that the biosensor discriminates tumor cells from healthy cells through the specific interaction between FA and folate receptors, as illustrated in Scheme 1. Besides, the electrodes' electrochemical response varied linearly with the logarithm of HeLa cells concentration, demonstrating their applicability in cancer diagnosis and predicting the tumor stage.

2. Materials and methods

2.1. Reagents

Polyallylamine hydrochloride (PAH), folic acid (FA), bovine serum albumin (BSA), potassium phosphate monobasic, dibasic sodium phosphate, sodium chloride, potassium chloride, potassium ferricyanide (III), potassium hexacyanoferrate (II) trihydrate, and sodium nitrate were acquired from Sigma-Aldrich. ITO substrates (surface resistance = 8–12 Ω) were purchased from Delta Technologies (USA). Eagle's Minimum Essential Medium (EMEM), fetal bovine serum, L-glutamine, and Trypsin/EDTA solution, were obtained from Vitrocell Embriolife. MCDB 131 Medium with no glutamine and trypan blue solution were purchased from Thermo Fisher Scientific. HeLa and HMEC cells were acquired from the Rio de Janeiro Cell Bank and stored at −80 °C after growth in cellular flasks. Tissue culture flasks (with areas of 25 cm^2, 75 cm^2, 175 cm^2) were acquired from Greiner-Silife. Phosphate buffered saline (PBS) at pH 8.0 was prepared using potassium phosphate monobasic 14 mM, sodium phosphate dibasic 87 mM, sodium chloride 136.7 M, and potassium chloride 2.7 mM. Phosphate buffer (PB) 100 mM pH 8.0 was prepared with potassium phosphate monobasic 61 mM and sodium phosphate dibasic 38 mM. Tris-HCl buffer 100 mM at pH 8.0 was prepared with Tris(hydroxymethyl)aminomethane (Sigma-Aldrich). The KCl 100 mM and $NaNO_3$ 100 mM solutions were both prepared at pH 8.0. All aqueous solutions were prepared using Milli-Q purified ultrapure water with 18.2 MΩ cm^{-1} resistivity.

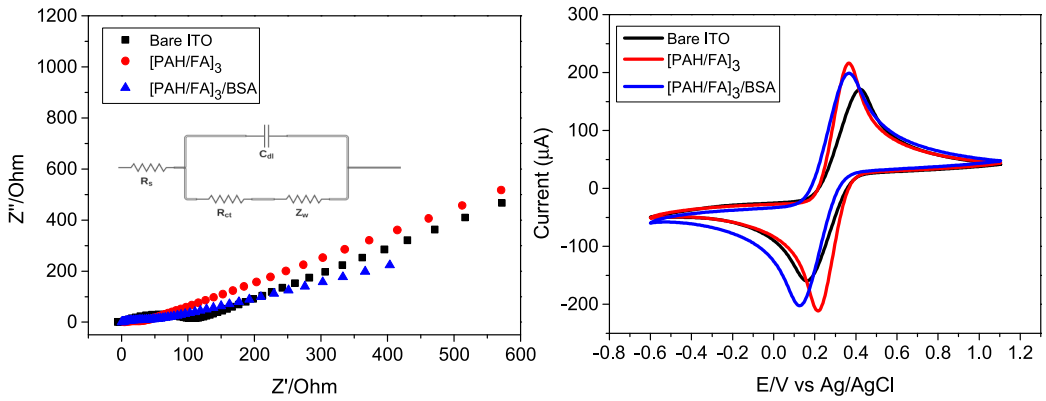

Fig. 1. Nyquist plots (A) and cyclic voltammograms (B) monitoring the fabrication steps of the LbL biosensor. The equivalent circuit best fitted to EIS data is showed in the inset (A). A 100 mM $NaNO_3$ solution was used as supporting electrolyte with 1 mM $[Fe(CN)_6]^{3-/4-}$ as redox probe. CV was performed with 100 mV s^{-1} scan rate.

2.2. Construction of LBL films

The growth of LbL PAH/FA films has been optimized and is described in detail in Ref. [29]. Briefly, after cleaning the ITO substrates, they were first immersed in the aqueous PAH solution (1 mg mL^{-1}) for 3 min, followed by washing in DI water (pH 6.0). The substrate pre-coated with PAH was then immersed in a FA solution (1 mg mL^{-1}, pH 8.0), followed by washing in water (pH 8.0). This self-assembly procedure was repeated three times to achieve a film with 3 PAH/FA bilayers.

2.3. Cell culture

HeLa and HMEC were cultured in EMEM and MCDB 131 complete medium (supplemented with 10% fetal bovine serum, and 200 μM L-glutamine) at 37 °C under a tension of 5% CO_2 until forming a cell monolayer. Cells were detached from the surface of the bottles using 0.05% trypsin-EDTA (Gibco), resuspended in complete medium, and washed with PBS by centrifugation at 1200 rpm for 4 min. Experiments were conducted with a minimum of 90% cell viability. After washing twice with buffer, the cells were counted with a Neubauer camera and the solutions were prepared with the following cell concentrations: 50, 1×10^2, 1×10^3, 1×10^4, 1×10^5, and 1×10^6 cells mL^{-1}.

2.4. Electrochemical measurements

Electrochemical measurements were carried out using a potentiostat/galvanostat model PGSTAT30 (Metrohm Autolab). A 100 mM $NaNO_3$ solution was used as supporting electrolyte and 1 mM $[Fe(CN)_6]^{3-/4-}$ was used as the redox probe. Cyclic voltmmetry (CV) and electrochemical impedance spectroscopy (EIS) measurements were taken in a conventional three-electrode electrochemical cell using ITO substrates (area = 50 mm^2) coated with 3-bilayer PAH/FA films as working electrodes, platinum plate (area = 50 mm^2) as auxiliary electrode, and homemade Ag/AgCl (KCl 3.0 M) as reference electrode. CV profiles were recorded in the −0.6 to 1.1 V potential range at 100 mV s^{-1} scan rate. EIS measurements were performed using 10 mV AC perturbation at open circuit potential, and the impedance was measured from 10 kHz to 0.1 Hz frequency range. The LOD was calculated based on IUPAC model, following the equation:

$$LOD = \frac{3\ x\ SD}{s}$$

where SD is the standard deviation calculated for three measurements performed in buffer and s is the slope obtained from analytical curve.

3. Results

3.1. LbL films assembly

The biosensor interface was prepared using the LbL self-assembly technique, as previously described [29]. Fig. 1 shows the electrochemical impedance spectra and the cyclic voltamograms of the electrode modification steps. After depositing the $[PAH/FA]_3$ film on the ITO surface, the charge transfer resistance (R_{CT}) decreases and the current increases. This change in the electrochemical properties occurs because the treatment of ITO electrodes with KOH solution makes them negatively charged, difficulting the electron transfer. However, the

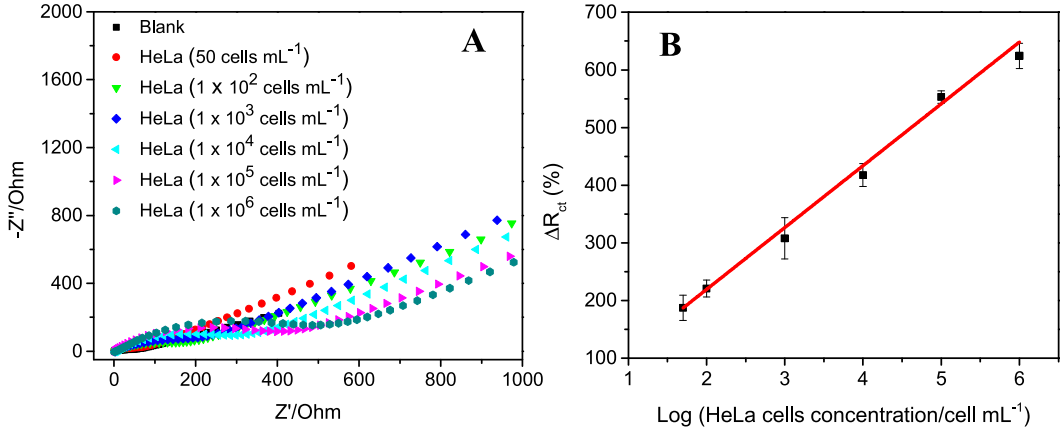

Fig. 2. (A) Impedance spectra (Nyquist plots) of the LbL-based biosensor at different HeLa cells concentration and (B) Analytical curve of normalized R_{CT} change (100 x $[R_{ct\ HeLa} - R_{ct\ blank}]/R_{ct\ HeLa}$) against the logarithm of HeLa cells concentration. Measurements in three independent electrodes (n = 3).

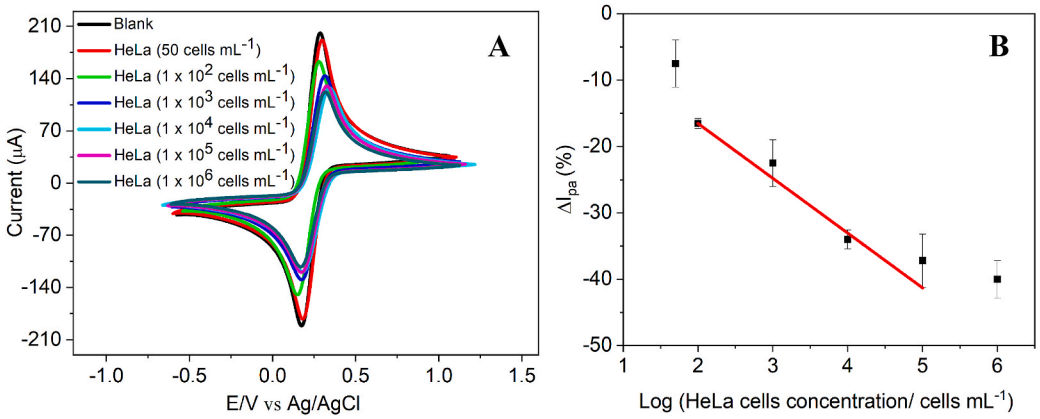

Fig. 3. (A) Cyclic voltammograms of the LbL-based biosensor at different HeLa cells concentration, (B) The analytical curve showing a linear relationship between the normalized I_{pa} change (100 x [$I_{pa\ HeLa} - I_{pa\ blank}$]/$I_{pa\ blank}$) and the logarithm of HeLa cells concentration. Measurements in three independent electrodes (n = 3). A 100 mM $NaNO_3$ solution was used as supporting electrolyte with 1 mM $[Fe(CN)_6]^{3-/4-}$ as redox probe. CV was performed with 100 mV s^{-1} scan rate.

Table 1
Analytical performance of electrochemical biosensors for tumor cells detection.

Analytical method	LOD (cells mL^{-1})	Linear range (cells mL^{-1})	Correlation coefficient	Cell line	Ref.
Square wave voltammetry	50	50–1.2 × 10^4	0.986	HT 29	[32]
Differential pulse voltammetry	10	10–10^6	Not reported	HeLa	[4]
Electro-chemiluminescent	3.5 × 10^3	3.5 × 10^3 – 3.5 × 10^5	0.996	HeLa	[33]
Differential pulse voltammetry	50	10^2–10^4	0.991	HeLa	[13]
Electrochemical impedance spectroscopy	4	50–1 × 10^6	0.994	HeLa	This work
Cyclic voltammetry	19	1 × 10^2–1 × 10^5	0.986	HeLa	This work

assembly of LBL film on the electrodes, protonates the hydroxyl groups on their surface. In addition, the electrochemical response obtained after blocking the biosensor with BSA is in agreement with other studies reported [30,31]. The equivalent electrical circuit best fitted to the impedance response was the Randles model (inset in Fig. 1A), which was used to calculate the R_{ct} of the EIS curves.

3.2. HeLa cells detection

To evaluate the electrochemical detection of HeLa cells, the biosensor was previously characterized in buffer solution (blank) by CV and EIS techniques and then incubated for 1 h in solutions containing HeLa cells at known concentrations. Upon incubation, CV and EIS measurements were again performed. As shown in the Nyquist plots (Fig. 2A), the R_{CT} increases with the tumor cell concentration, indicating that the tumor cells interact with the electrode surface. The analytical curve (Fig. 2B) shows a linear relationship between the normalized R_{ct} change (100 x [$R_{ct\ HeLa} - R_{ct\ blank}$]/$R_{ct\ HeLa}$) and the logarithm of HeLa cells concentration in the range from 50 to 1 × 10^6 cells mL^{-1}. The equation obtained by linear regression from EIS measurements in three independent electrodes was $\Delta R_{ct} = 4.82 + 107.25 \times \log_{10}$ (HeLa cells concentration/cells mL^{-1}) with a correlation coefficient (R^2) of 0.994. The standard deviation of normalized R_{ct} change for three independent electrodes was 22% and the developed biosensor exhibited a low limit of detection of ~4 cells mL^{-1}.

For CV measurements, a decrease in the biosensor current was observed as the concentration of HeLa cells increased (Fig. 3A), corroborating the impedance results. The analytical curve showed that the normalized change of the anodic peak current (100 x [$I_{pa\ HeLa} - I_{pa\ blank}$]/$I_{pa\ blank}$) is inversely proportional to the logarithm of HeLa cells concentration (Fig. 3B). The linear relationship (in the range from 1 × 10^2 to 1 × 10^5 cells mL^{-1}) follows the equation $\Delta I_{pa} = -0.05 - (8.25 \times \log_{10}$ (HeLa cells concentration/cells mL^{-1}) with $R^2 = 0.986$. The standard deviation of normalized I_{pa} change for three independent electrodes was 3.55% and the limit of detection using the CV technique

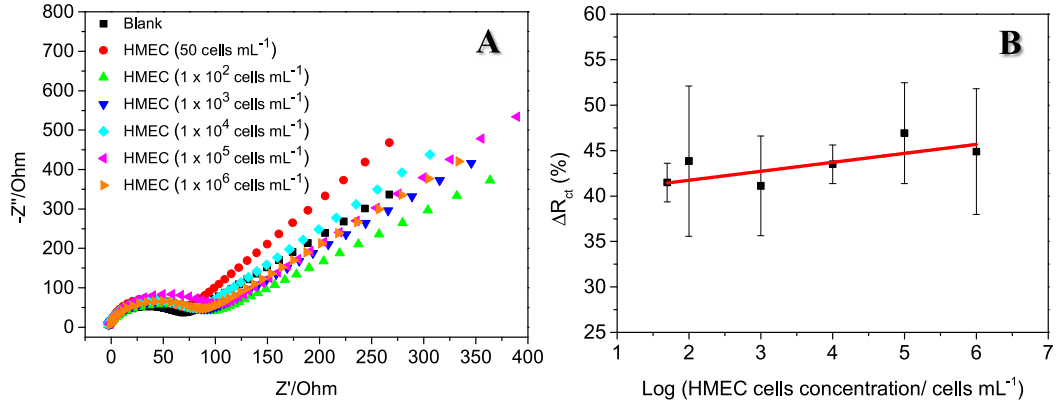

Fig. 4. Selectivity assay of the LbL-based biosensor: (A) Nyquist plots showing the impedance response at different concentrations of HMEC cells. (B) Normalized R_{CT} change (100 x [$R_{ct\ HMEC} - R_{ct\ blank}$]/$R_{ct\ HMEC}$) as a function of HMEC cells concentration.

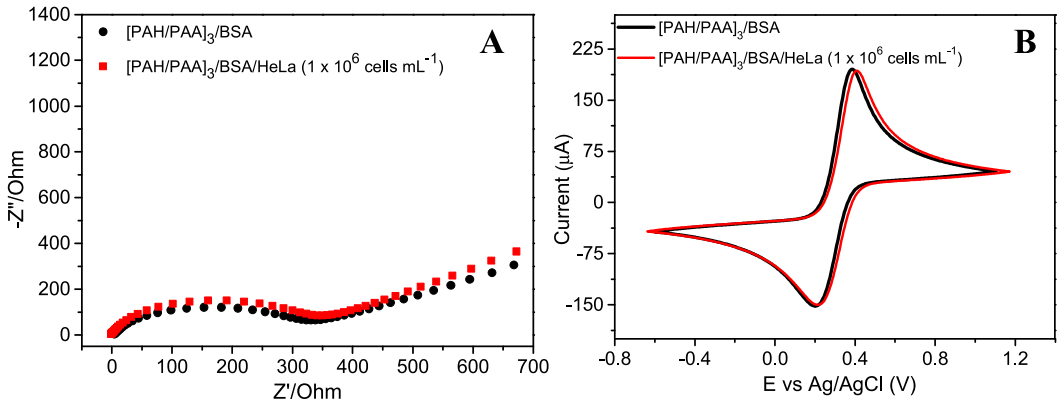

Fig. 5. The electrochemical response of the ITO electrode modified with $[PAH/PAA]_3$ LbL film to HeLa cells: (A) Impedance spectra and (B) cyclic voltammograms. A 100 mM $NaNO_3$ solution was used as supporting electrolyte with 1 mM $[Fe(CN)_6]^{3-/4-}$ as redox probe. CV was performed with 100 mV s^{-1} scan rate.

was 19 cells mL^{-1}.

The results show that the LbL-based biosensor presents an excellent electrochemical response as a function of the concentration of HeLa cells, which demonstrates its potential application for the quantification of tumor cells. Comparing the CV and EIS techniques, it is observed that the impedance measurements presented higher sensitivity and more accurate results. More importantly, the limit of detection reached by our biosensor using the EIS technique is much lower than that reported by other biosensors [4,13,14,16] and shows that this device can also be used to detect cancer in early stages. In Table 1, the analytical performance of the LbL-based biosensor is compared with others.

3.3. Selectivity

To evaluate the selectivity of our detection system to FR-positive tumor cells, the biosensors were submitted to electrochemical measurements after being incubated for 1 h with HMEC cells in the same tested concentrations of HeLa cells. As shown in Fig. 4A, the impedance response of the biosensor is not significantly dependent on the concentration of non-tumor cells. Although there is a change in R_{CT} compared to the blank measurement, it is observed in the analytical curve (Fig. 4B) that there is a very subtle change in average values of ΔR_{ct} (%) for the range of 50 –1 × 10^6 cells mL^{-1}, which suggests that this increase is caused by the non-specific adsorption of some cells on the electrode surface. At the lowest concentration tested, the ratio between the ΔR_{ct} (%) for tumor cells and that for normal cells ($\Delta R_{ct\ HeLa}/\Delta R_{ct\ HMEC}$) is almost 4 and increases to 14 when the concentration is 1 × 10^6 cells mL^{-1}. These results demonstrate that the biosensor distinguishes tumor cells from healthy cells even at low concentrations with a good signal difference.

The high selectivity of the biosensor can be attributed to the FRα overexpression on the surface of tumor cells, allowing them to interact with the FA-modified electrode surface. To confirm this hypothesis, ITO electrodes were modified with the LbL assembly of PAH and the PAA (not containing FA), forming a $[PAH/PAA]_3$ multilayer film. These electrodes without the recognition molecule (FA) were incubated for 1 h in HeLa cells suspension (1 × 10^6 cells mL^{-1}). As shown in Fig. 5, no significant changes were observed in EIS (Figura 5A) and CV (Figura 5B) measurements after incubation, indicating that the electrodes modified with the $[PAH/PAA]_3$ films are not able to capture the tumor cells. This behavior demonstrates that the detection and quantification of tumor cells are due to the binding of FRα to FA molecules on the electrode surface.

3.4. Reproducibility and repeatability

The reproducibility of the biosensor was evaluated after each of the following steps: after LbL assembly of the films, after blocking with BSA, and after detection of HeLa cells at a concentration of 1 × 10^6 cells mL^{-1}. Three independent electrodes were constructed at the same conditions and submitted to CV and EIS measurements. Table S1 (Supporting information) shows the average value of the oxidation current, standard deviation (SD), and relative standard deviation (RSD) calculated between the electrodes. The results of the CV measurements demonstrate a good reproducibility of the biosensor in the 3 studied steps, with RSD of 3.89% for the detection test.

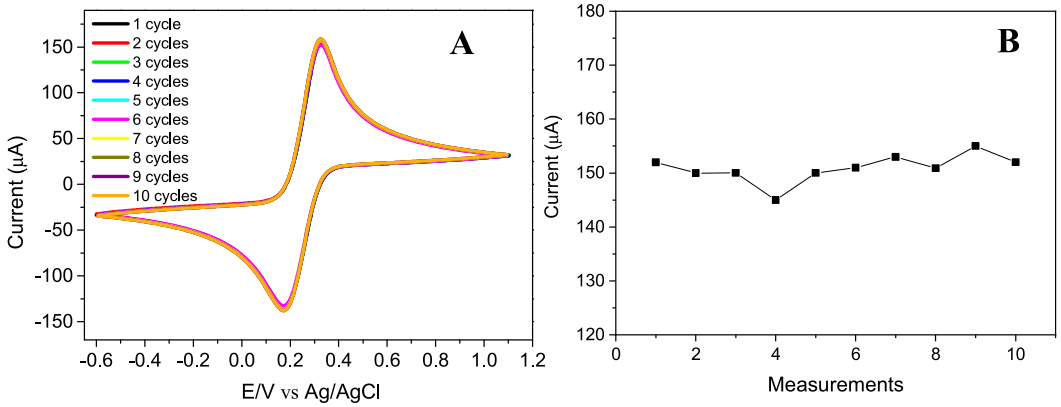

Fig. 6. Biosensor repeatability: cyclic voltammongrams (A) and oxidation current values (B) obtained for 10 successive measurements of the biosensor after incubation with HeLa cells (1 × 10^6 cell mL^{-1}). A 100 mM $NaNO_3$ solution was used as supporting electrolyte with 1 mM $[Fe(CN)_6]^{3-/4-}$ as redox probe. CV was performed with 100 mV s^{-1} scan rate.

For impedance analysis, the biosensor exhibited an excellent reproducibility, as shown in Table S2 (Supporting information). Very low RSD values of 1.7% were obtained for the blocking and detection steps. These results highlight the LbL-based biosensor's performance, presenting high electrode-to-electrode reproducibility with better RSD values than those reported in the literature for other cytosensors [4,13].

Finally, the repeatability of measurements on the same electrode was evaluated after incubation with HeLa cells at 1×10^6 mL^{-1} cells. Fig. 6 shows the cyclic voltammograms and oxidation current values for 10 successive measurements. A minor variation is observed and the calculated RSD was 1.8%, showing the excellent repeatability of the developed biosensor.

4. Conclusions

LbL-based biosensors were successfully applied to the selective detection of tumor cells through the specific interaction between the folate receptors on the cell surface and the FA molecules immobilized onto the electrode. The biosensor exhibited a linear electrochemical response to the concentration of tumor cells and an excellent sensitivity was achieved, with LOD of 4 cells mL^{-1} and 19 cells mL^{-1} using EIS and CV techniques, respectively. Furthermore, the biosensors presented great reproducibility (RSD = 1.7%) and repeatability (RSD = 1.8%). In addition to their excellent analytical performance, the LbL-based biosensors are fabricated using a simple and low-cost methodology which makes them promising to be applied as cancer cells detection systems.

Declaration of competing interest

The authors declare that they have no known competing financial interests or personal relationships that could have appeared to influence the work reported in this paper.

Acknowledgments

We gratefully acknowledge to the Conselho Nacional de Desenvolvimento Científico e Tecnológico - CNPq (Grant numbers 158754/2015-8 and 133505/2016-2) and São Paulo Research Foundation - FAPESP (Grant numbers 2018/07508-3 and 2018/12670-4) for the financial support and the researchers from Nanomedicine and Nanotoxicology Group for their cooperation in our studies.

Appendix A. Supplementary data

Supplementary data to this article can be found online at https://doi.org/10.1016/j.talanta.2021.122506.

Credit author statement

Abilene Rodrigues Correa: Conceptualization, Methodology, Validation, Writing – review & editing; Isabella Sampaio: Validation, Formal analysis, Methodology, Writing – original draft, Writing – review & editing; Edson José Comparetti: Methodology; Writing – review & editing; Nirton Cristi Silva Vieira: Conceptualization, Methodology, Writing – review & editing, Funding acquisition, Supervision; Valtencir Zucolotto: Conceptualization, Writing – review & editing, Funding acquisition, Supervision.

References

[1] F. Bray, J. Ferlay, I. Soerjomataram, R.L. Siegel, L.A. Torre, A. Jemal, Global Cancer Statistics 2018: GLOBOCAN Estimates of Incidence and Mortality Worldwide for 36 Cancers in 185 Countries, 2018, https://doi.org/10.3322/caac.21492.

[2] M. Rahman, D. Cui, S. Zhou, A. Zhang, D. Chen, A graphene oxide coated gold nanostar based sensing platform for ultrasensitive electrochemical detection of circulating tumor DNA, Anal. Methods. 12 (2020) 440–447, https://doi.org/10.1039/c9ay01620a.

[3] K. Brindle, New approaches for imaging tumour responses to treatment, Nat. Rev. Canc. 8 (2008) 94–107, https://doi.org/10.1038/nrc2289.

[4] J. Liu, Y. Qin, D. Li, T. Wang, Y. Liu, J. Wang, E. Wang, Highly sensitive and selective detection of cancer cell with a label-free electrochemical cytosensor, Biosens. Bioelectron. 41 (2013) 436–441, https://doi.org/10.1016/j.bios.2012.09.002.

[5] S. Damiati, M. Peacock, R. Mhanna, S. Søpstad, U.B. Sleytr, B. Schuster, Bioinspired detection sensor based on functional nanostructures of S-proteins to target the folate receptors in breast cancer cells, Sensor. Actuator. B Chem. 267 (2018) 224–230, https://doi.org/10.1016/j.snb.2018.04.037.

[6] D.J. O'Shannessy, G. Yu, R. Smale, Y.S. Fu, S. Singhal, R.P. Thiel, E.B. Somers, A. Vachani, Folate receptor alpha expression in lung cancer: diagnostic and prognostic significance, Oncotarget 3 (2012) 414–425, https://doi.org/10.18632/oncotarget.519.

[7] M. Scaranti, E. Cojocaru, S. Banerjee, U. Banerji, Exploiting the folate receptor α in oncology, Nat. Rev. Clin. Oncol. 17 (2020) 349–359, https://doi.org/10.1038/s41571-020-0339-5.

[8] T. Yang, F. Xu, D. Fang, Y. Chen, Targeted proteomics enables simultaneous quantification of folate receptor isoforms and potential isoform-based diagnosis in breast cancer, Sci. Rep. 5 (2015) 16733, https://doi.org/10.1038/srep16733.

[9] A. Cheung, H.J. Bax, D.H. Josephs, K.M. Ilieva, G. Pellizzari, J. Opzoomer, J. Bloomfield, M. Fittall, A. Grigoriadis, M. Figini, S. Canevari, J.F. Spicer, A. N. Tutt, S.N. Karagiannis, Targeting folate receptor alpha for cancer treatment, Oncotarget 7 (2016) 52553–52574, https://doi.org/10.18632/oncotarget.9651.

[10] J. Soleymani, M. Hasanzadeh, M.H. Somi, N. Shadjou, A. Jouyban, Probing the specific binding of folic acid to folate receptor using amino-functionalized mesoporous silica nanoparticles for differentiation of MCF 7 tumoral cells from MCF 10A, Biosens. Bioelectron. 115 (2018) 61–69, https://doi.org/10.1016/j.bios.2018.05.025.

[11] G.M. Van Dam, G. Themelis, L.M.A. Crane, N.J. Harlaar, R.G. Pleijhuis, W. Kelder, A. Sarantopoulos, J.S. De Jong, H.J.G. Arts, A.G.J. Van Der Zee, J. Bart, P.S. Low, V. Ntziachristos, Intraoperative tumor-specific fluorescence imaging in ovarian cancer by folate receptor-α targeting: first in-human results, Nat. Med. 17 (2011) 1315–1319, https://doi.org/10.1038/nm.2472.

[12] C.R. Fischer, C. Müller, J. Reber, A. Müller, S.D. Krämer, S.M. Ametamey, R. Schibli, [18F]fluoro-deoxy-glucose folate: a novel PET radiotracer with improved in vivo properties for folate receptor targeting, Bioconjugate Chem. 23 (2012) 805–813, https://doi.org/10.1021/bc200660z.

[13] J. Ni, Q. Wang, W. Yang, M. Zhao, Y. Zhang, L. Guo, B. Qiu, Z. Lin, H.H. Yang, Immobilization free electrochemical biosensor for folate receptor in cancer cells based on terminal protection, Biosens. Bioelectron. 86 (2016) 496–501, https://doi.org/10.1016/j.bios.2016.07.012.

[14] Y. Lin, X. Huang, Y. Zhang, D. Chen, J. Wang, F. Luo, L. Guo, B. Qiu, Z. Lin, Electrochemiluminescence biosensor for the detection of the folate receptor in HeLa cells based on hyperbranched rolling circle amplification and terminal protection, ChemElectroChem 6 (2019) 827–833, https://doi.org/10.1002/celc.201801094.

[15] R. Ranjan, E.N. Esimbekova, V.A. Kratasyuk, Rapid biosensing tools for cancer biomarkers, Biosens, Bioelectron 87 (2017) 918–930, https://doi.org/10.1016/j.bios.2016.09.061.

[16] L. Du, W. Chen, J. Wang, W. Cai, S. Kong, C. Wu, Folic acid-functionalized zirconium metal-organic frameworks based electrochemical impedance biosensor for the cancer cell detection, Sensor. Actuator. B Chem. 301 (2019) 127073, https://doi.org/10.1016/j.snb.2019.127073.

[17] T. Tian, L. Li, Y. Zhang, H. Liu, L. Zhang, M. Yan, J. Yu, Dual-mode fluorescence biosensor platform based on T-shaped duplex structure for detection of microRNA and folate receptor, Sensor. Actuator. B Chem. 261 (2018) 44–50, https://doi.org/10.1016/j.snb.2018.01.129.

[18] H.H. Cai, J. Pi, X. Lin, B. Li, A. Li, P.H. Yang, J. Cai, Gold nanoprobes-based resonance Rayleigh scattering assay platform: sensitive cytosensing of breast cancer cells and facile monitoring of folate receptor expression, Biosens. Bioelectron. 74 (2015) 165–169, https://doi.org/10.1016/j.bios.2015.06.012.

[19] G. Wang, X. He, L. Wang, X. Zhang, A folate receptor electrochemical sensor based on terminal protection and supersandwich DNAzyme amplification, Biosens. Bioelectron. 42 (2013) 337–341, https://doi.org/10.1016/j.bios.2012.10.066.

[20] J.R. Siqueira, L. Caseli, F.N. Crespilho, V. Zucolotto, O.N. Oliveira, Immobilization of biomolecules on nanostructured films for biosensing, Biosens. Bioelectron. 25 (2010) 1254–1263, https://doi.org/10.1016/j.bios.2009.09.043.

[21] J.J. Richardson, J. Cui, M. Björnmalm, J.A. Braunger, H. Ejima, F. Caruso, Innovation in layer-by-layer assembly, Chem. Rev. 116 (2016) 14828–14867, https://doi.org/10.1021/acs.chemrev.6b00627.

[22] R.M. Iost, F.N. Crespilho, Layer-by-layer self-assembly and electrochemistry: applications in biosensing and bioelectronics, Biosens. Bioelectron. 31 (2012) 1–10, https://doi.org/10.1016/j.bios.2011.10.040.

[23] M.L. Moraes, N.C. de Souza, C.O. Hayasaka, M. Ferreira, U.P. Rodrigues Filho, A. Riul, V. Zucolotto, O.N. Oliveira, Immobilization of cholesterol oxidase in LbL films and detection of cholesterol using ac measurements, Mater. Sci. Eng. C 29 (2009) 442–447, https://doi.org/10.1016/j.msec.2008.08.040.

[24] S. Wu, J. Hao, S. Yang, Y. Sun, Y. Wang, W. Zhang, H. Mao, X.M. Song, Layer-by-layer self-assembly film of PEI-reduced graphene oxide composites and cholesterol oxidase for ultrasensitive cholesterol biosensing, Sensor. Actuator. B Chem. 298 (2019) 126856, https://doi.org/10.1016/j.snb.2019.126856.

[25] Y. Si, J.W. Park, S. Jung, G.S. Hwang, Y.E. Park, J.E. Lee, H.J. Lee, Voltammetric layer-by-layer biosensor featuring purine nucleoside phosphorylase and chitosan

for inosine in human serum solutions, Sensor. Actuator. B Chem. 298 (2019) 126840, https://doi.org/10.1016/j.snb.2019.126840.
[26] C. Cong, K. Bian, X. Zhang, L. Luo, L. Li, H. He, C. Li, Q. Zhao, S. Wang, Z. Hao, Y. He, D. Gao, Sensitive measurement of tumor markers somatostatin receptors using an octreotide-directed Pt nano-flakes driven electrochemical sensor, Talanta 208 (2020) 120286, https://doi.org/10.1016/j.talanta.2019.120286.
[27] J. Zhou, J. Tang, G. Chen, D. Tang, Biosensors and Bioelectronics Layer-by-layer multienzyme assembly for highly sensitive electrochemical immunoassay based on tyramine signal ampli fi cation strategy, Biosens. Bioelectron. 54 (2014) 323–328, https://doi.org/10.1016/j.bios.2013.11.032.
[28] E.B. Aydın, M.K. Sezgintürk, Indium tin oxide (ITO): a promising material in biosensing technology, TrAC Trends Anal. Chem. (Reference Ed.) 97 (2017) 309–315, https://doi.org/10.1016/j.trac.2017.09.021.
[29] A.R. Correia, I. Sampaio, E.J. Comparetti, N.C.S. Vieira, V. Zucolotto, Optimized PAH/Folic acid layer-by-layer films as an electrochemical biosensor for the detection of folate receptors, Bioelectrochemistry 137 (2020) 107685, https://doi.org/10.1016/j.bioelechem.2020.107685.
[30] L.C. Brazaca, C.B. Bramorski, J. Cancino-bernardi, S. Cruz-machado, R.P. Markus, B.C. Janegitz, An antibody-based platform for melatonin quantification, Colloids Surf. B Biointerfaces 171 (2018) 94–100, https://doi.org/10.1016/j.colsurfb.2018.07.006.
[31] M. Li, B. He, Ultrasensitive sandwich-type electrochemical biosensor based on octahedral gold nanoparticles modified poly (ethylenimine) functionalized graphitic carbon nitride nanosheets for the determination of sulfamethazine Ming, Sensor. Actuator. B Chem. (2020) 129158, https://doi.org/10.1016/j.snb.2020.129158.
[32] J. Soleymani, M. Hasanzadeh, M.H. Somi, N. Shadjou, A. Jouyban, Highly sensitive and specific cytosensing of HT 29 colorectal cancer cells using folic acid functionalized-KCC-1 nanoparticles, Biosens. Bioelectron. 132 (2019) 122–131, https://doi.org/10.1016/j.bios.2019.02.052.
[33] H. Jiang, X. Wang, Label-free detection of folate receptor (+) cells by molecular recognition mediated electrochemiluminescence of CdTe nanoparticles, Anal. Chem. 86 (2014) 6872–6878, https://doi.org/10.1021/ac501734x.